PERFORMANCE OPTIMIZATION OF INTERACTING SAILS THROUGH FLUID STRUCTURE COUPLING

V.G. Chapin[1], N. de Carlan[1, 2], P. Heppel[2]

[1]Institut Supérieur de l'Aéronautique et de l'Espace, Université de Toulouse, France
[2]Peter Heppel & Associates, Port-Louis, France

SUMMARY

In this paper, the problem of sailing yacht rig design has been addressed through the development of a computational framework based on viscous Computational Fluid Dynamic (CFD) modelling for the aerodynamic part and on a non linear structural modelling for the structure part. The Fluid Structure Interaction (FSI) coupling used is a loose coupling. The interest but also the expertise needed to use Reynolds Averaged Navier-Stokes (RANS) equations for the aerodynamic modelling is justified through examples and validations with a focus on complex separated flow configurations. The originality of the presented computational framework is its ability to address complex, non linear optimization problems with a derivative free evolutionary strategy. This capability is enhanced by the fact that it is based on a remeshing technique rather than on a deforming mesh one. After the description of the main elements of this computational framework for Fluid Structure Interaction, it is used for generic sail optimization problems and for the rig design of a 18 footer to illustrates its capabilities and limitations to produce accurate aeroelastic solutions on sailing yacht rigs.¶

NOMENCLATURE

α_i	Entry angle of the sail
β	Apparent wind angle
C, c	Sail chord
C_d	Drag coefficient
C_l	Lift coefficient
Cl_{max}	Maximum lift coefficient
C_h	Heeling force coefficient
C_r	Driving force coefficient
C_p	Pressure coefficient
D	Drag force
δ	Sail trim angle
δ*	Optimal sail trim angle
δ_m	Mainsail trim angle
δ_f	Foresail trim angle
f/c	Sail camber
f /c*	Optimal sail camber
F_h	Heeling force
F_r	Driving force
g	Overlap (longitudinal distance between the jib clew and the mast)
i	Angle of attack = β-δ
i*	Optimal angle of attack = β-δ*
L	Lift force
L/D	Lift-to-drag ratio
$(L/D)_{max}$	Maximum lift-to-drag ratio
M_c	Heeling moment
S	Sail surface
x_f/c	Chord-wise coordinate of the maximum camber
V_A	Apparent wind velocity

1. INTRODUCTION

The design of interacting sails for highly competitive sailing yachts is a multidisciplinary design problem addressed by sail designers, sailors and scientists over many years [1-3]. Sail design is an art using considerations from membrane structures and aerodynamics. The sail designer wishes to have a better knowledge of the global three-dimensional flow around sails with particular attention on wakes and peculiar phenomena linked to rig layout. He/she is interested in obtaining a quantitative analysis of aerodynamic loads and structural stresses and their dependency on design changes. This is part of the design process.

Historically, many papers have addressed a part of these questions from various scientific points of view [1-5]. This research has shed some light on sail design questions and their main parameters such as sail aspect ratio, camber, entry angle, optimal angle of attack, sail interaction, mast effect, coupling mechanism between the mainsail and the foresail, upwind and downwind sailing conditions, sail twist and atmospheric boundary layer, flow separation, fluid structure interaction, *etc*...

In a more general sense, this membrane design problem is a complex multidisciplinary problem at the crossroads of the research developments needed in fluid structure coupling with numerous fields of application. This complex and multidisciplinary problem implies that various approaches are currently in development with various hypotheses. Rigorous comparisons between each of them are of great benefit in promoting a critical mind in a community where passion is sometimes dominant.

For the aerodynamic part of the FSI problem, some existing tools are based on inviscid modelling [6, 7] and some are based on viscous flow modelling [8, 9, 10].

Velocity Prediction Programs (VPP) that are frequently used in sailing yacht design are based on empirical aerodynamic and hydrodynamic models to predict aero-hydrodynamic forces and their dependences to design parameters. These models are crude representations of the real forces acting on sailing yachts [11-15]. Some of their drawbacks are known to result in some misleading predictions but increasing their performance is not easy [11-15]. As said before by Korpus [16], experiments are probably the best method to predict these forces by taking into account real world effects like viscous separation, unsteadiness, *etc*… However, it is difficult to discard scale effects during the transposition to real yachts. In that direction, full-scale measurements have been recently performed [17]. It is always difficult to take into account aero-structural coupling which is one of the main factors in sail design. Another difficulty specific to experiments is the ability to access all physical variables needed to better understand flow around bodies which may be helpful to guide future design.

The best aerodynamic model we have today is viscous CFD through RANS simulations [16, 18-23]. RANS codes have two drawbacks when used to predict forces acting on a yacht. They may be time-consuming and they need some expertise to be accurate. However, the greatest time consuming task in the process is the engineer time needed to generate meshes with a high quality standard on complex geometries. These facts drive two questions to make RANS methods useful for yacht and sail designers:

- Is it possible to automate mesh generation and integrate RANS simulations into a user-friendly environment?
- Is it possible to validate RANS predictions by comparisons with experiments representative to real flow conditions?

These questions have been addressed in previous papers [21, 22] by developing a computational framework *ADONF* for two-dimensional aerodynamic problems. It has been shown that it is possible to resolve the optimization problem about sail design and sail interactions by simulating a large number of flow configurations through high-fidelity RANS solver. Examples illustrated have been focused on questions like: how to better design and trim interacting sails, or complex rigs? How to maximize a given function like driving force chosen to evaluate the sailing boat performance and taking into account some constraints like the maximum heeling moment?

In this paper the extension of the computational framework *ADONF* is proposed to address three-dimensional FSI problem.

The fluid model is briefly presented in its main components and key elements for accurate results. The structural model is described with special attention to the fluid structure interfacing methods used. The computational framework and the optimization algorithm are also described. Then examples are used to illustrate capabilities of the computational framework *ADONF* for sail design and optimization with an FSI formulation for three-dimensional flows.

2. FLUID MODEL

In this section, main elements of the computational model are described. Fluid dynamics equations used to simulate the flow around interacting sails are presented with the solver and physical models and limitations. RANS equations have been resolved on hybrid meshes with structured and unstructured mesh and conformal or non-conformal interfaces between domains [19]. The hybrid mesh strategy is a powerful technology which increases flexibility to generate high quality meshes around interacting sails for two and three-dimensional flows [19].

2.1 SOLVER

The solver used for the resolution of the Navier-Stokes equations in most of the paper is Fluent 6.3 except in section 7.5 where OpenFOAM 1.6 is used. FLUENT is a steady or unsteady, compressible or incompressible, three-dimensional solver which resolves the previously given RANS equations. In the present study, the incompressible version with segregated solver and the Spalart-Allmaras turbulence model [24] with standard constants have been used. Second-order spatial schemes were used and second-order temporal schemes were used for unsteady simulations. The usefulness of second-order scheme will be illustrated in the result section.

To solve the Navier-Stokes equations, proper boundary conditions are required on all frontiers of the flow domain. At the wall boundaries, the no-slip condition is applied. A pressure outlet boundary condition is applied at the outlet. A symmetry boundary condition is used on the top and bottom faces of the domain. A velocity inlet boundary condition is applied on other frontiers (inlet, leeward and windward) with a background turbulence level of 1%. For Three-dimensional simulations, a uniform wind without atmospheric boundary layer profile is used for the inlet condition.

2.2 MESH ISSUES

The mesh generation is a crucial step in the process of RANS simulation. It is a time consuming activity which needs engineer experience and long practice to rigorously clean the CAD geometry and to make the best choice for the mesh topology and generation. The mesh influence on the results on typical sails configurations may be important and should be carefully evaluated and bounded by relevant choices in mesh size and distribution over the flow domain.

Boundary layers have to be resolved on bodies (mast and sails) and this imposes some criteria on mesh size in the normal and tangential direction to the walls. Flow gradients should be well resolved. This may be a difficult task on typical sails because of the zero thickness and the subsequent leading-edge pressure gradient when there is no mast and the angle of attack is not ideal. Based on these constraints, hybrid mesh technology may be a critical issue for high-fidelity RANS simulations [19].

In fact, results are never totally independent of the chosen mesh. The relevant question when interpreting RANS results on sails is: how bounded is the mesh influence on physical quantities of interest and the required precision? This should be investigated on a simplified geometry through validation with wind-tunnel results [19].

To illustrate the mesh convergence, Figure 1, the lift-to-drag ratio (C_l/C_d) convergence with mesh nodes on a typical sail (f/c = 12.5%, Reynolds number Re = 1.4 x 10^6) calculated on four meshes have been shown. On this particular example, a good convergence on a critical physical quantity may be observed.

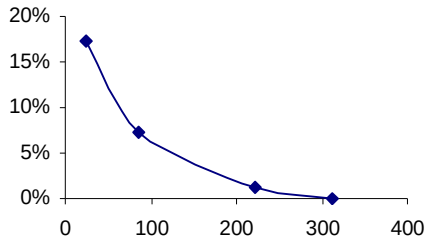

Figure 1: lift-to-drag ratio normalized by the finest mesh value convergence with mesh refinement (nodes number divided by 1000)

Another important feature of meshes is their flexibility to be used with different kinds of sail geometries and trim angles. A critical point for yacht rig aerodynamic studies is the necessity to generate meshes on multiple bodies (mast, mainsail, jib, *etc*…) which interact and may be displaced relative to each other. The challenge is to generate good quality meshes in the boundary layer regions of each body without using too high aspect ratio cells which may generate numerical scheme instability and too many grid points for computational efficiency reasons. To respect these topologic constraints and obtain good mesh control, hybrid meshes (Figure 2) is a useful technology. For more flexibility, it may be completed by non conformal interface between the inner structured region around masts and sails and the outer unstructured region around all interacting structured domains (Figure 2) as was done with Gambit [25]. The mast trailing-edge with link to the zero-thickness sail is a region of difficulty for the structured mesh part and needs much more attention and some tricks.

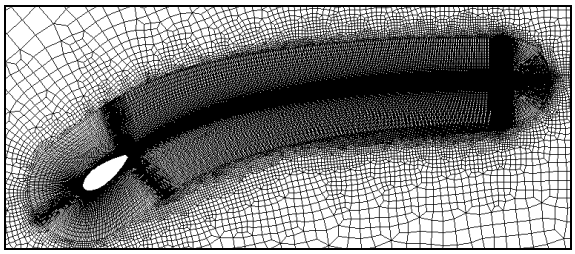

Figure 2: hybrid mesh example

2.3 TURBULENCE MODELING

Sail aerodynamics is highly concerned with separation bubble, turbulent transition and the turbulent reattachment process and it is well known that these phenomenon and their associated pressure losses may have a critical influence on pressure and friction distribution on sails. Also an accurate representation of laminar and turbulent separated flow regions is critical when we are concerned with drag prediction.

In [19] detail flow analysis with separation bubble, turbulent transition and turbulent reattachment process on various mast and mainsail configurations have been computed for validation purposes. Comparisons were made with wind-tunnel results of Wilkinson [26-28]. It has been shown that the one equation Spalart-Allmaras turbulence model may have coherent qualitative behaviour on mast-sail geometries and may show to be better than more sophisticated turbulence models based on two transport equations.

Hence all simulations presented in this paper are based on the use of the Spalart-Allmaras turbulence model. Concerning mesh considerations, the model is used in its low Reynolds number form for two-dimensional RANS simulations (y+<5) or with wall functions with y+~30 for three-dimensional RANS simulations or y+~300 for three-dimensional RANS or FSI optimizations.

It has been shown that RANS modelling with a careful application of best practices is able to predict qualitatively main flow features of these two-dimensional flows. A similar validation process of RANS modelling on three-dimensional sail flow configurations is challenging and still needs to be done.

3. STRUCTURE MODEL

The structural modelling is based on the software RELAX. It is an interactive, fully non-linear finite-element code to analyse fabric structures using a state of the art relaxation method. RELAX's special sail analysis features enables it to be used to predict the behaviour of almost any large-displacement structures [29]. It is a good candidate for sail analysis through a fluid-structure loop.

The method of resolution is based on Barnes studies [30], using dynamic relaxation and kinematic damping. The model is based on membrane elements

for sail modelling and beam elements for battens. This model is described by a parametric surface (u,v local coordinates). The sail materials can be described as a composite material: each ply contains a filament laid or a film. The behaviour of the material can be non linear. The resolution method is based on an explicit scheme with a first order time and space discretization.

RELAX has a sophisticated meshing tool which can automatically mesh sail geometry given by a CAD software, such as RHINO 3D. Sail meshing is realized using Delaunay triangulation. The grid relates to boundaries of panels and is refined in regions of greatest curvature. During analysis the nodes move to their new equilibrium position. There is no remeshing of the structure.

Knowing that a membrane element has no resistance in compression, a wrinkling model is implemented in RELAX to take into account the compressive stresses. As a membrane has an infinite number of kinematics degree of freedom (possibility to deform without a change of stress) and a grid has a finite number of kinematics degrees, the wrinkling modelling allows a better prediction by adding degrees of freedom. At that time, the membrane is considered as an orthotropic material with a linear behaviour.

RELAX is a robust solver but excess material which is not supported by a batten is a source of instability. This is a consequence of the choice of membrane elements which have no resistance in bending. Also, extended foot modelling can be problematic.

The RELAX interface presents various possibilities for trimming. This is useful to modify the sail shape in a realistic way. In particular, halyard, stay and clew lengths can be changed, as carriage location.

All data are saved from the last analysis. This is a useful point in the case of an FSI loop. From a loop to the next one, just the pressure field has to be updated, while stresses, geometry and the mesh are conserved in the memory by the software. This allows a saving in computing time.

4. FLUID STRUCTURE COUPLING

With actual computing power and accessibility of specialized software, it is now possible to predict the flying shape of sails through FSI coupling [8]. The resolution in the same time of aerodynamic and structural equations is the best way to achieve this goal but it is a computationally expensive way [31]. A loose coupling method allows a reasonable prediction with smallest resources by using specialized software for the fluid and the structural part.

4.1 PRINCIPLE

In a loose coupling method, aerodynamic and structural equations are solved independently. It is possible to use two different sets of software, one dedicated to structural analysis and the other dedicated to fluid analysis, even if they are not developed to communicate together. Once the loop is initialized with the sail design shape and an arbitrary constant pressure field, the structural code sends the sail displacements to the fluid code and the fluid code sends back the pressure field on the sail surfaces to the structural code. Iterations are made until convergence.

4.2 INTERFACING

The aerodynamic and structural solvers are different and don't have the same needs concerning the meshing. Their respective meshes are different and independent and an efficient interfacing method needs to be developed to link these modules. In the FSI loop, the aerodynamic solver sends the pressure field on the geometry to the structural solver and the structural solver communicates the new shape of the geometry resulting from the given pressure field. Also, it is necessary to provide a mapping of the pressure field from the fluid mesh to the structural mesh with no prior knowledge of the target mesh.

To achieve this, the coordinate of the structural surface is mapped onto the unit square using a development of the texture-mapping method described in Desbrun [32].

When the structural mesh geometry is exported for CFD, we also save a record of the relation between the texture-map coordinates and the current global Cartesian coordinates. We do this by constructing a NURBS surface approximating the structural model with surface parameterization chosen to match the texture coordinates. This provides a good record of the relation between global Cartesian and texture coordinates, although the tensor product NURBS surface cannot capture all the shape details. This NURBS surface is saved in a neutral CAD format.

The CFD typically returns a surface pressure field at global Cartesian positions of the fluid mesh. For each pressure sample point, we associate the pressure value to texture coordinates by finding the closest point on the NURBS surface. This operation is loss-less because every pressure sample is mapped. It introduces position errors of second order relative to the error of the NURBS approximation.

Then the new sail shape corresponding to this pressure field is given by the structural solver using an IGES file. The new sail shape is used by the aerodynamic mesher to generate a new mesh instead of using a grid moving technique. This choice is more time consuming than moving grid techniques but it is more robust for large displacement membranes and small cells necessary on sail boundary layers for accurate pressure field prediction. The CPU time necessary to automatically generate a new mesh is about 10% of the total simulation time.

4.3 LIMITS

This type of loose coupling FSI is not a perfect solution [31]. Maintaining accuracy in data exchanges between structural and aerodynamic software is important to obtain relevant aeroelastic results. Stability can also be a problem, in particular when aerodynamic stiffness and structural stiffness are of the same order. Tests and comparisons are necessary to evaluate different coupling techniques.

5. COMPUTATIONAL FRAMEWORK

Fluid motion around deforming and interacting sails in their real environment is a complex non linear problem. This may be more complex if separated flow sail configurations with unsteady phenomena related to deformations and wrinkling are considered. Because there are a lot of parameters that define a complete rig design, there is a crucial need to integrate and automate the entire simulation process. If this is done, it will be easier to understand flow physics and gain insight for better rig design and trim. Turnaround time of the simulation process is a major constraint in common use software. *ADONF* is a response to this problem. It gives us the ability to analyse or optimize a large number of rig configurations. It opens a new way to the design process by using a computational framework. It provides a method to enhance the classical design process, which is rather based on the designer experience and a trial and error process, by a computational design process able to explore the design space through the resolution of an optimization problem.

ADONF is a computational framework which integrates and automates the entire computational environment for flow simulation from CAD definition, to mesh generation, flow simulation, flow analysis and design modifications using an optimization loop. This optimization loop is symbolically described in Figure 3. The main bottleneck is the mesh generation process automation. However, it is also a critical advantage over hand made mesh generation as it generates meshes of high reliability and reproducibility. This specific property of automated meshes increases the ability to compare and rank different sail designs and trims.

As will be shown through examples in the next section, it becomes possible to investigate and resolve new questions about fluid motion around designed bodies and their related performances. The first level of new questions that can be investigated is the "what-if" questions. What will be the performance of this rig design if I change the mast section? What will be the performance of this rig if I change the genoa overlap, g, preserving a constant sail surface, S? *Etc*… Only the sail designer's imagination and time limits the number of what-if questions.

For the second level of questions, optimization algorithms have been implemented in *ADONF*. With optimization algorithms, a second set of questions becomes open for sail researchers or sail designers. How to change the rig design or the deck plan to increase the performance of that particular sailing boat in given wind conditions? How to change rig trimming to increase boat speed in given wind conditions? What is the best camber and trim of these two interacting sails to maximize driving force or driving to heeling force ratio? *Etc*… This will be illustrated in more detail through examples in the results sections.

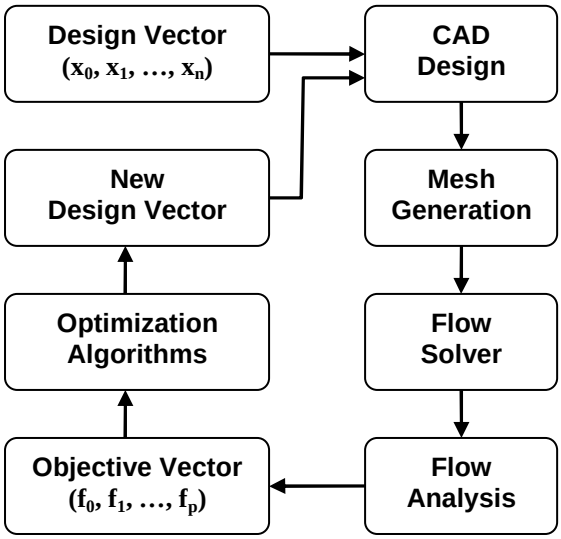

Figure 3: *ADONF* optimization diagram

6. OPTIMIZATION ALGORITHM

Many optimization algorithms may be used depending on the properties of the objective function in the explored design space. Gradient or simplex methods are well known optimization algorithms. They have been used but they have some disadvantages. They may be slow to converge close to the optimum and this may be a problem when the evaluation cost of the objective function is high. This is precisely the case for CFD applications. Another disadvantage is the zigzag down valley problem, but the more important problem is their dependence on initial conditions for multi-modal optimization problems. It is not easy to show if a given CFD problem may have a multi-modal objective function when the objective function evaluation is high and the number of design variables is large [33]. However in a simple optimization problem in CFD with a subset of the total design variables it has been shown that the objective function may be multi-modal [21]. It is one of the reasons we have chosen to use an evolutionary strategy rather than more conventional ones.

An evolution strategy (ES) is an optimization method based on Darwinian ideas of the natural evolution. These techniques, created in the early 1960s, have been developed further for fluid flow problems in the 1970s and later [34].

In this work, CMA-ES (**C**ovariance **M**atrix **A**daptation - **E**volution **S**trategy) an evolutionary algorithm is used in most of the paper except in section 7.2 and 7.3 where a gradient based algorithm is used. It is well adapted for non linear non convex optimization problems in a continuous domain. It is also well adapted for noisy problems when derivative based methods fail. Because it doesn't presume or require the existence of a derivative of the objective function, it is feasible on non-smooth and even non-continuous problems, as well as on multi-modal problems. Following Hansen [35] it is a particularly reliable and highly competitive evolutionary algorithm for local optimization and also for global optimization problems [36, 37]. One more advantage of using CMA-ES is that it doesn't require a tedious parameter tuning for its application as opposed to commonly used genetic algorithms.

Now we have defined all the ingredients of our computational framework, examples will be given to illustrate the possibility it opens up for sailing yacht rig optimization through an aerodynamic or an aeroelastic modelling of the problem.

7. RESULTS

Results will be presented in five sections. The first section illustrates the importance of viscous flow modelling through RANS. The second, third and fourth sections illustrate the interest of optimization studies for sails. The fifth section illustrates FSI applications.

7.1 VISCOUS FLOW PREDICTION

A first point about viscous flow modelling is to understand why and when it is needed for sail and rig performance prediction, design and optimization.

To illustrate this point, it may be that three-dimensional sails should be considered. In this case, one may refer to the Jones [38] study as an illustrative example. In the paper, it is shown on an IACC rig with a mainsail and a jib that viscous and inviscid solutions predict opposite rankings for two sail camber design in same wind conditions. It will be of interest to know which modelling is right but there are no experimental results given. Probably RANS is the right solution because it takes into account one more important physical phenomenon, the viscous effects. Hence, viscous drag is taken into account. However more critically, with RANS modelling, pressure drag associated with flow separation may be qualitatively predicted as shown in a previous paper on sail sections with detailed comparisons to the Wilkinson wind-tunnel tests [19]. A few results from this paper are used in this section to illustrate the abilities and limitations of RANS modelling for sail flows.

Let us look in more details a simple case with only one two-dimensional sail. RANS prediction is more demanding in mesh resolution and CPU time than panel methods, also this should not be underestimated. Because sail camber is an important sail design parameter, highly related to flow separation and pressure drag, the ability of RANS modelling to predict variations of sail aerodynamic performances for various sail cambers has been evaluated.

In Figures 4 and 5 the maximum lift coefficient Cl_{max} and the maximum lift-to-drag ratio $(L/D)_{max}$ are presented as functions of sail camber for RANS simulations conducted over a range of angles of attack with first and second order numerical schemes. It is interesting to note that, for both schemes, RANS predicts a saturation of Cl_{max} with f/c. The maximum Cl_{max} value obtained for f/c ranging from 25% to 30% can't be surpassed by increasing the sail camber as is known by experiments [39]. This is related to flow separation which is qualitatively well predicted by RANS and not by inviscid methods [19, 40]. This is not to say that the maximum Cl_{max} value predicted by RANS is highly accurate but that RANS is sufficient to detect a trade-off on the sail camber design parameter. This is a major difference between the inviscid and the viscous model.

In the same way, accurate RANS modelling with a second-order scheme is able to predict that there is an optimum camber value which maximizes $(L/D)_{max}$ as shown in wind-tunnel experiments [20] and as Bethwaite observed on sea tests [39]. The value of the predicted optimum camber agrees with the Bethwaite experimental values (10%-13%). The accurate prediction of the maximum $(L/D)_{max}$ may be dependent on the numerical choices made for the simulation (mesh resolution, numerical scheme, *etc*…) and need expertise. Best practices should be defined [40] and more detailed validation conducted for accurate prediction. As an example, for a given mesh, the influence of the numerical scheme used is illustrated for a sail with various camber values in Figure 5. On this figure, the second-order scheme is able to predict an optimum camber value but the first order scheme doesn't. This example clearly illustrates that when conducting RANS simulations around sails, an important best practice is to use second-order numerical schemes rather than first-order ones. For more details on best practices to predict the right qualitative behaviour of lift and drag force coefficients as functions of sail camber, angle of attack, mast diameter, see following references [19, 20]. Best practices should also be considered when conducting more complex simulations around three-dimensional sails or rigs.

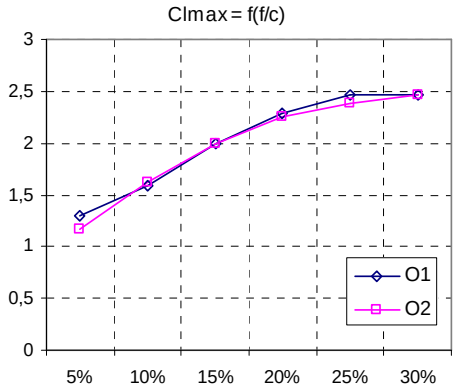

Figure 4: Cl_{max} versus f/c ranging from 5% to 30%. (O1) first-order scheme, (O2) second-order scheme

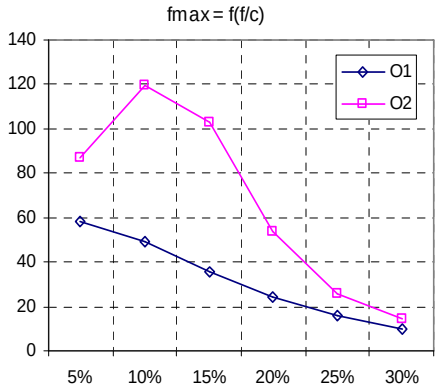

Figure 5: $(L/D)_{max}$ versus f/c ranging from 5% to 30%. (O1) first-order scheme, (O2) second-order scheme

7.2 OPTIMAL SINGLE SAIL

From Bethwaite [39], it is known that there exists an optimum sail camber for a given mast. This observed fact has been chosen as a test case to validate *ADONF* and the implemented optimization algorithms for sail design questions. For a single sail, the optimization problem may be formulated as follows: for a given apparent wind angle, what is the optimal camber and related trim angle which maximize the driving force Fr? The apparent wind angle chosen was $\beta = 30°$ a typical value for upwind conditions. Other sail parameters are listed in the following table:

Table 1: sail parameters of the optimization problem

x_f	C	$(f/c)_0$	δ_0
30%	6500	7%	13°

A gradient based algorithm, known as the Simplex method, is used. The optimization problem has been resolved by computing solutions based on the RANS model. The computation of twenty designs has been sufficient to obtain a good convergence of the sail camber, f/c, and trim angle, δ (Figure 6a, 6b, 7). The following optimal solutions for maximum driving force and maximum lift-to-drag ratio have been found:

Table 2: results of the 2 optimization problem resolved

Objective	(f/c)*	δ*
Max(Fr)	18%	22°
Max(L/D)	8%	27°

The number of RANS simulations needed to determine the optimal solution is dependent on the number of variables. In this example with only two variables, the convergence to the optimal solution is fast. It has been verified, by changing the initial condition, that the optimal solution was independent to the initial condition. An example of algorithm convergence is given in Figures 6 & 7 for the two parameters: camber, trim angle and the objective function driving force.

It is interesting to note that the optimal solution, maximizing the driving force, presents a separation point near the trailing-edge on the suction surface (Figure 8). This clearly illustrates the ability of viscous CFD to make a trade-off, between high lift by high camber and high angle of attack and low drag by low flow separation on the suction side of the sail, through RANS simulations.

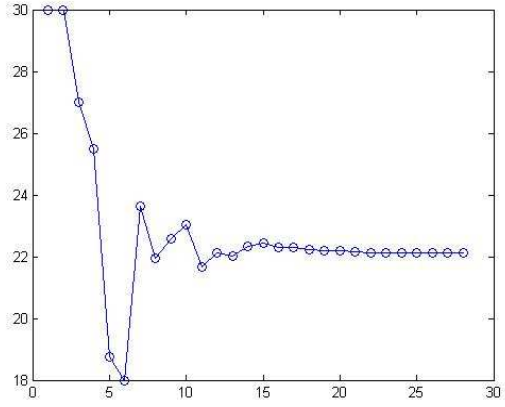

Figure 6a: convergence of the trim angle δ versus the number of explored design

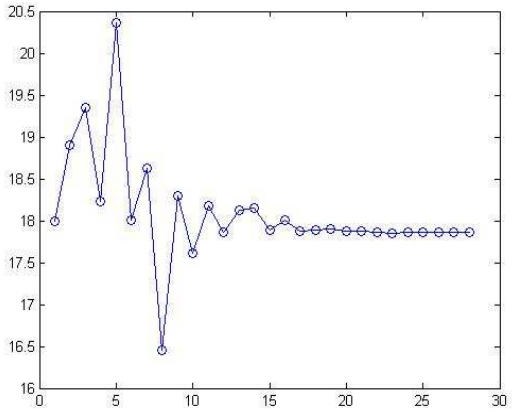

Figure 6b: convergence of the sail camber f/c versus the number of explored design

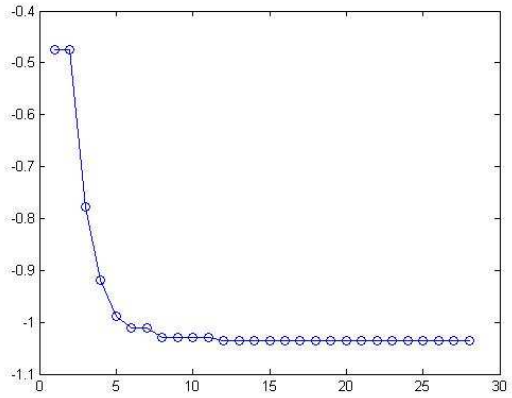

Figure 7: convergence of the driving force coefficient Cr versus the number of explored design

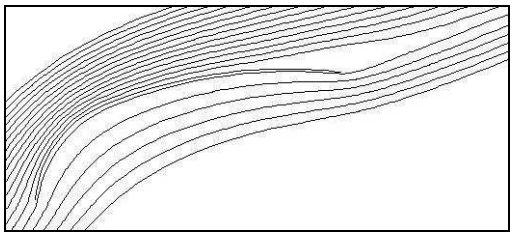

Figure 8: streamlines around the sail for maximum driving force at $\beta = 30°$

7.3 OPTIMAL INTERACTING SAILS

A more challenging optimization problem is the interacting sails problem. The mainsail-jib interaction on a sailing boat is a well known problem which has generated long debates and controversies [1, 41]. The question was to know if *ADONF* may be useful to explore the sail interaction problem in more detail and contribute to clarifying the relation between foresail and mainsail shapes and rig performance by taking into account separated flows through RANS modelling.

The optimization problem may be formulated as follows: for a given apparent wind angle, what are the optimal cambers and related trim angles for mainsail and jib which maximize the driving force, Fr, of the complete rig? The apparent wind angle chosen was $\beta = 30°$.

As in the single sail optimization, the Simplex algorithm has been used. The results for the optimum camber & trim angle are listed in the following table:

Objective	$(f/c)_m$*	$(f/c)_f$*	δ^*_m	δ^*_f
Max(Fr)	27%	30%	3°	32°
Max(Fr/Fh)	4%	19%	10°	31°

The solution that maximizes the driving force is visualized in Figure 9. As in the previous case, small separation regions are found near the trailing-edge on the suction surfaces.

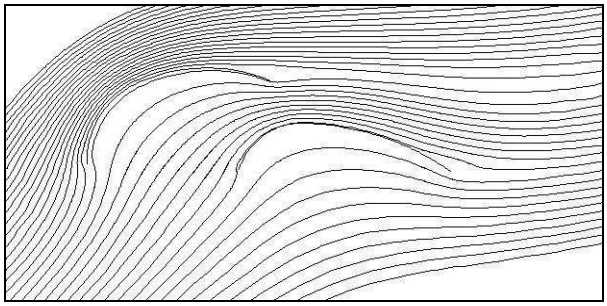

Figure 9: stream function around two interacting sails for maximum driving force at $\beta = 30°$

For further investigation, and more realistic or useful results for a given boat, it will be necessary to extend *ADONF* to three-dimensional sails optimization and possibly to take into account a constraint on the heeling moment. This constraint may be added through a penalty method or another constraint handling method [37, 42]. The extension to three-dimensional flows and fluid-structure interaction is underway [43] as may be seen in the next sections. Validations of *ADONF* results on interacting sails through wind-tunnel test comparisons will be useful but are hard to do without experimental results in the open literature.

7.4 3D SAIL DESIGN OPTIMIZATION

Our computational framework *ADONF* has been extended to three-dimensional optimization. As a first example of a three-dimensional aerodynamic optimization based on RANS simulations a generic mainsail in upwind conditions is considered.

The sail optimization problem is defined as follows: search to maximize the driving force of the sail through a parameterization of its camber and trim angle on its three main sections (bottom, middle and top sections). This defines a mono objective and six variables optimization problem (O1P6). In this first example no FSI loop is implemented yet. The

optimization process resolves the three-dimensional Navier-Stokes equations in RANS formulation with the Spalart-Allmaras turbulence model and the CMA-ES evolutionary algorithm search for optimal cambers and trim angles in the three sail sections.

The mesh is automatically generated on GAMBIT with sail surface boundary layer resolution of y+=O(300) and a total of 125 000 cells. This is a coarse but sufficient mesh resolution to test the optimization as was shown during previous tests. The resolution constraint may be relaxed during optimization because, as noted above, automatic mesh generation has a high repeatability. Another reason is that we just need to rank various sail shapes, not to predict their absolute performance. In fact, as shown in a previous paper, the important point is to be sure that main flow features of the explored rig configurations are qualitatively well predicted [19]. At the end of the process, when the best shape is found, it is always possible to increase the mesh resolution during another RANS simulation for higher absolute accuracy.

During the optimization process, which in this small case has been stopped at 91 RANS simulations, all the sail designs tested are represented in the design space and in the performance space. The history of the optimization process may be followed. As an example, in Figure 10, the aerodynamic performance of all the tested configurations is represented in the (Cl, Cl/Cd) plane. Because the optimization search for maximum lift coefficient, an accumulation of tested design is clearly visible in the maximum lift coefficient region during the end of the optimization. When you see that and you think it is enough, it is time to stop the optimization process.

A subset of designs, the non-dominated designs, separates the aerodynamic performance plane in two regions (Figure 10). On the left of the Pareto frontier, we see the region of accessible designs and on the right, the region of inaccessible designs (for the given optimization problem). The non-dominated solutions along the Pareto frontier gives the best compromises achievable in the plane (Cl, Cl/Cd) with the parameterized sail studied during this optimization problem.

The friction lines (lines tangent to the friction vector on the wall surface) on the leeward side of the sail for selected designs extracted during the optimization are shown on Figure 11. On the two first sail designs, separation zones are clearly identified at the top of the sail for design 1 and in the mid-section on design 2. On the following sail design 3 the flow is more attached along nearly all the sail surface with only a very small separation at the top of the sail. Design 4 is the optimal design found at the end of the optimization. This optimal sail design shows no separated zones. It maximizes the driving force in the range tested for camber and trim angle ($4\%<f/c<40\%$, $5°<\delta<25°$). It may be noted that the optimal three-dimensional sail, as opposed to two-dimensional optimal sails, found by the ES optimization, is not far from a separated flow but is not separated.

Given optimization examples in two and now in three-dimensional flows illustrates what can be done on sail design with the computational framework *ADONF*. It may be used to quantify the influence of mainsail-jib overlapping factor, sail camber position, entry and exit angles, *etc*, in a simple manner or to find the optimal design based on a given objective function and design constraints.

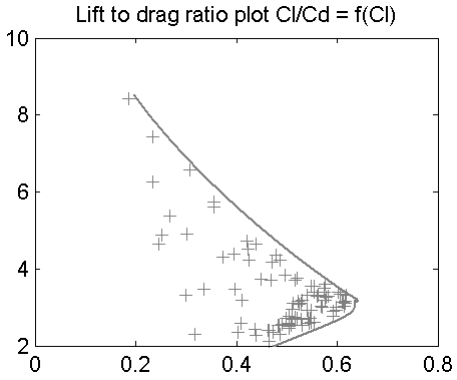

Figure 10: aerodynamic performances of all the tested sail designs during the optimization process in the plane (lift, lift-to-drag ratio).

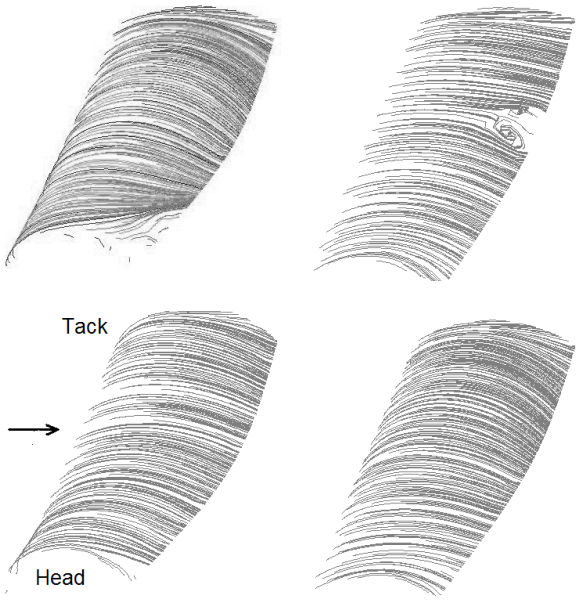

Figure 11: selected sail designs before the convergence toward an optimal sail design.

7.5 PRELIMINARY FSI RESULTS

7.5.1 FSI ANALYSIS

As a first FSI analysis, we are considering the flow around a genoa alone in upwind conditions. This genoa design is taken first to quantify the influence of the aerodynamic model on the resultant flying sail

shape and the influence of the structural model on the aerodynamic loads for two apparent wind angles (30°, 33°).

Figure 12 gives a comparison of three sail shapes: the design shape in grey, the flying shape given by RELAX with a constant pressure distribution resulting in the same aerodynamic force and the flying shape given by RELAX with a pressure field obtained by a three-dimensional RANS calculation. Regions of differences may be observed. The luff and leech regions are important regions of differences with a high dependence of the sail entry angle to the tension of the forestay. This will be seen in more details in the next section.

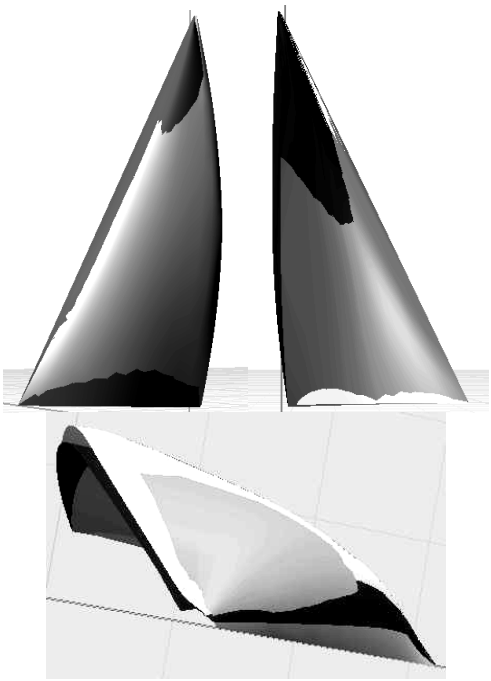

Figure 12: design shape (grey), flying shape / RANS (white), flying shape / uniform pressure (black), (left) leeward side (right) windward side (bottom) top view

Figures 13 and 14 give a comparison of the friction lines along leeward genoa surface for two apparent wind angles (30°, 33°) on the design shape and on RANS flying shape.

Figure 13, shows that the flow doesn't separate on the leeward side of the sail for the lower apparent wind angle but it may be observed that separation is not far away. Always in Figure 13, at the higher apparent wind angle, separation takes place on the lower part of the sail. For RANS converged flying shapes, it is seen in Figure 14, that the flow separates for both apparent wind angles. Separation is present only in the middle part for the lower apparent wind angle. Extension of the separation region is far larger for the higher apparent wind angle. This last case is nearly totally separated on the leeward side of the genoa.

The separation extension on the sail surface has an impact on driving and heeling forces. On design shapes, the driving force increases by 10% when the apparent wind angle increases by 3° despite the separation which takes place on 20% of the sail surface. On flying shapes, the driving force is decreased by 20% when the apparent wind angle is increased by 3° because of the total three-dimensional separation on the leeward side of the genoa. These four visualizations of the leeward side of the genoa clearly illustrate the relative importance of aerodynamic and structural effects that may take place on sails.

Figure 15 shows friction lines on the windward side of the genoa for both apparent wind angles on the flying shapes calculated by RANS-FSI. This sail side is simpler to analyse with no strong non linear phenomena except on the bottom part of the genoa with the tip vortex (Figure 16) and the top part with a high vertical velocity component along the stay which is more pronounced on the head part of the sail. This vertical component is very high for the highest apparent wind angle with a totally separated flow on the leeward side (Figure 15).

It will be interesting to observe these flow fields on the genoa in the interaction with a mainsail to have a finer understanding of the interaction consequences on the three-dimensional flow fields.

All these figures clearly show the interest of three-dimensional FSI simulations. With these detailed flow fields, it becomes possible to increase our global understanding of three-dimensional viscous flows, to observe the emergence of separated regions with design parameters variations and to quantify their consequences on aerodynamic forces and sail performances.

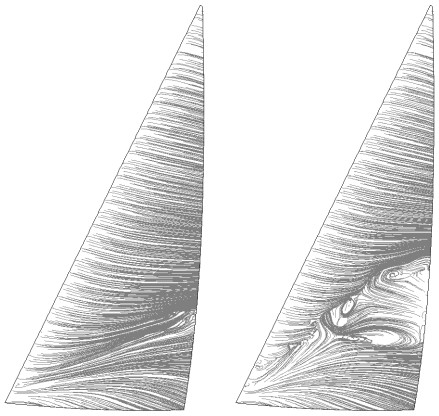

Figure 13: leeward design shape: β = 30°, 33°

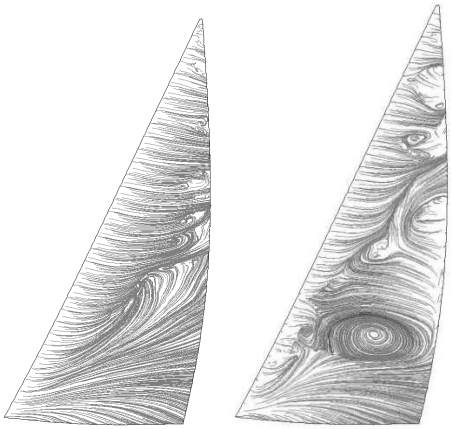

Figure 14: leeward flying shape: β = 30°, 33°

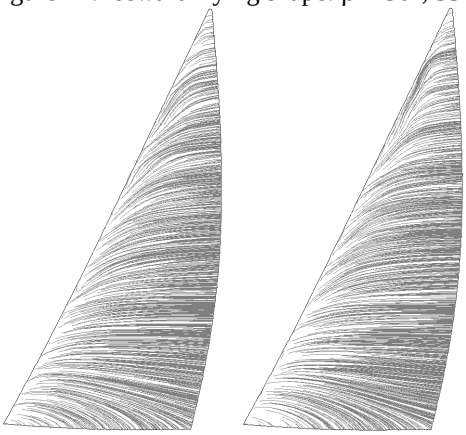

Figure 15: windward flying shape: β = 30°, 33°

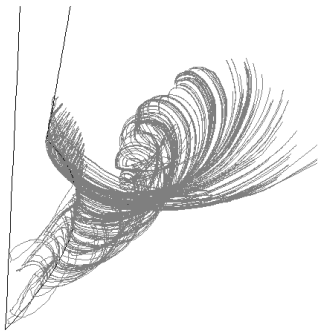

Figure 16: tip vortex on the bottom of the genoa β = 30°

7.5.2 18 FOOTER RIG DESIGN

As a second step in the FSI investigation, the influences of main parameters have been quantified on the design of an 18 footer genoa in upwind sailing conditions (apparent wind V_A=20 knots, β=21°). A mainsail and a genoa are modelled but the fluid-structure interaction was studied only for the genoa. The mainsail was considered as a rigid sail (Figure 17). The genoa is first designed with all its geometric characteristics: seams, stripes, filaments, battens, reinforcements. Rhino 3D has been used to create this first model (Figure 18). Mechanical characteristics are applied on each part of the sail using RELAX.

Figure 17: 18 footer rig

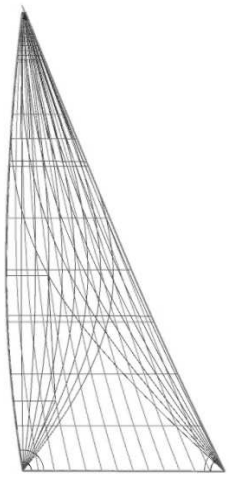

Figure 18: genoa design with all its geometric characteristics.

In this example, after only three iterations of the FSI loop between the structural and the aerodynamic codes the convergence is good, with less than a centimetre of difference between the two last sail shapes and less than 1% on driving and heeling forces between the two last iterations (see following table).

Aerodynamic loads convergence in SI units with FSI iterations:

	It.	Fr	Fh	Fr/Fh
Design shape	0	316	952	0.33
Flying shape	1	313	1077	0.29
“	2	305	1051	0.29
“	3	302	1045	0.29

The first difference between the design shape and the flying shape concerns the fullness of the sail: the sail moves downwind, the forestay bends, the leech opens and the twist changes (Figure 19). Considering what happens at the 20%, 40%, 60% and 80% heights of the sail, it can be seen in figure 20 that the flying shape is less twisted than the design shape, with smaller camber, and a camber position which moves forward.

Quantifications of these differences on sail shape are given in the following table:

	20%	40%	60%	80%
δ	11° - 14°	19° - 14°	24° - 16°	30° - 18°
f/c	8 – 7	13 – 10	17 – 13	20 – 15
x_f/c	39 – 38	33 – 28	35 – 26	40 – 27
α_i	44° - 46°	68° - 63°	79° - 70°	86° - 71°

The difference between global aerodynamic loads on the design and flying shapes is about 5% for the driving force and 10% for the heeling force. In this case, sail deformation decreases sail performances.

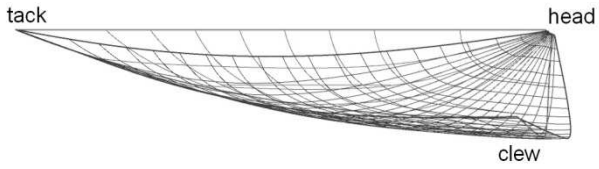

Figure 19: design shape (grey) and flying shape (dark grey)

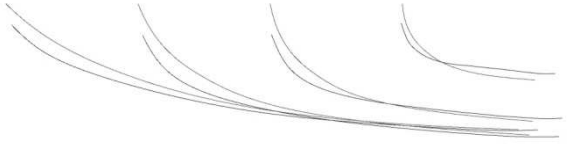

Figure 20: four sail cuts of the design and flying shapes

8. CONCLUSIONS

ADONF, a new computational framework for the analysis, design and optimization of flows around sails through RANS modelling has been extended to three-dimensional flows and fluid structure interaction in collaboration with Peter Heppel Associates. First results obtained in FSI mode have been presented.

The main results are as follows:

- The importance of RANS modelling for optimization studies has been emphasized due to its ability to predict aerodynamic performance trade-off of sails in relation to flow separation.
- On a single sail section, it has been shown that the resolution of an optimization problem based on RANS modelling is able to determine that there is an optimal camber as found in wind-tunnel tests and sea tests and that the optimal camber obtained is in the relevant range observed.
- On two interacting sail sections, it has been shown that the resolution of an optimization problem based on RANS modelling is able to determine the respective optimal camber and trim for both sail sections.
- For the first time, a six parameter optimization problem has been resolved to determine the best three-dimensional sail shape and trimming to maximize the driving force.

Additional results are as follows:

- A user-friendly environment to run a large number of RANS simulations and to resolve multidisciplinary optimization problems about sail flows has been developed.
- A high-fidelity RANS solver with hybrid meshes has been validated for sail sections and is able to capture main flow features like separated flows on mast and mainsail configurations [19].
- A derivative free optimization algorithm based on evolutionary strategy implemented in *ADONF* for the search of optimal rigs for complex multi-modal rig configurations has been developed.
- A loose coupling FSI loop between a RANS based aerodynamic solver and RELAX a non linear structural solver has been developed.

ADONF as a multidisciplinary computational framework based on RANS modelling opens new possibilities for sail flow analysis and optimization. In the future, more detailed results and validations through wind-tunnel test comparisons on three dimensional sails or rigs will be conducted.

9. ACKNOWLEDGMENT

This paper is an extended and corrected version of the following paper: Chapin V.G., de Carlan N. & Heppel P., "Performance optimization of interacting sails through fluid structure coupling", Innov'Sail 2010, Lorient, France.

10. REFERENCES

1. Gentry A., "The Aerodynamics of Sail Interaction", *3th AIAA Symposium on the Aero/Hydronautics of Sailing*, Redondo Beach, California, USA, November 1971.
2. Gentry A., "A Review of Modern Sail Theory", *11th AIAA Symposium on the Aero/Hydronautics of Sailing*, Seattle, Washington, USA, September 1981.
3. Marchaj C. A., *Aero-Hydrodynamics of Sailing*, USA, 1980.
4. Milgram J.H., "Sail Force Coefficients for Systematic Rig Variations", SNAME technical & research report R-10, September 1971.

5. Milgram J.H., “Effects of Masts on the Aerodynamics of Sail Sections”, Marine Technology, vol. 15(1), 35-42, 1978.

6. Shankaran, S., Jameson, A. and Margot Gerritsen, "Numerical Analysis and Design of Upwind Sails", 21st AIAA Applied Aerodynamics Conference, AIAA Paper AIAA-2003-3498, Orlando, FL, June 23-26, 2003.

7. Augier B, Bot P., Hauville F., Durand M., “Experimental Validation of Unsteady Models for Wind Sails Rigging Fluid Structure Interaction”, *INNOVSail2010, Innovation in high performance sailing Yacht*, Lorient, France, May 2010.

8. Renzsch H., Graf K., “FlexSail – A Fluid Structure-Interaction Program for the Investigation of Spinnakers”, *INNOVSail2008, Innovation in high performance sailing Yacht*, Lorient, France, May 2008.

9. Paton J., Morvan H., Heppel P., “Fluid Structure Interaction of Yacht Sails”, *INNOVSail2008, Innovation in high performance sailing Yacht*, Lorient, France, May 2008.

10. Trimarchi D, Turnock S.R., Taunton J.T., Chapelle D., “Performance The use of Shell Elements to capture sail wrinkles and their influence on aerodynamic loads”, *INNOVSail2010, Innovation in high performance sailing Yacht*, Lorient, France, May 2010.

11. Claughton A., “Development in the IMS VPP Formulations”, *SNAME 14th Chesapeake Sailing Yacht Symposium*, Annapolis, USA, 1999.

12. Fossati F., Muggiasca S., Viola I.M., Zasso A., “Wind Tunnel Techniques for Investigation and Optimization of Sailing Yachts Aerodynamics”, *Proceeding of the 2nd High Performance Yacht Design Conference*, Auckland, February 2006.

13. Jackson P.S., “An improved upwind sail model for VPPs”, SNAME 15th *Chesapeake Sailing Yacht Symposium*, Annapolis, USA, 2001.

14. Oossanen P. van, “Predicting the Speed of Sailing Yachts”, SNAME Transactions, Vol 101, 337-397, 1993.

15. Teeters J., Ranzenbach., Prince M., “Changes to Sail Aerodynamics in the IMS Rule”, *SNAME 16th Chesapeake Sailing Yacht Symposium*, Annapolis, Maryland, USA, March 2003.

16. Korpus R., “Performance Prediction without Empiricism: A RANS-Based VPP and Design Optimization Capability”, *SNAME 18th Chesapeake Sailing Yacht Symposium*, Annapolis, Maryland, USA, March 2007.

17. Viola I.M. & Flay R.G.J., “Full-scale Pressure Measurements on a Sparkman & Stephens 24-foot Sailing Yacht”, Journal of Wind Engineering and Industrial Aerodynamics, Vol. 98, pp. 800–807, 2010.

18. Korpus R., “Reynolds Averaged Navier-Stokes in an Integrated Design Environment”, *MDY04 International Symposium on Yacht Design and Production*, Madrid, Spain, 2004.

19. Chapin V. G., Jamme S. and Chassaing P., “Viscous CFD as a relevant decision-making tool for mast-sail aerodynamics”, *Marine Technology*, **42**(1), p1-10, 2005.

20. Chapin V. G., Neyhousser R., Jamme S. Dulliand G., Chassaing P., “Sailing Yacht Rig Improvements through Viscous CFD”, *SNAME 17th Chesapeake Sailing Yacht Symposium*, Annapolis, Maryland, USA, March 2005.

21. Chapin V. G., Neyhousser R., Dulliand G., Chassaing P., “Analysis, Design and Optimization of Navier-Stokes Flows around Interacting Sails”, *MDY06 International Symposium on Yacht Design and Production*, Madrid, Spain, March 2006.

22. Chapin V. G., Neyhousser R., Dulliand G., Chassaing P., “Design Optimization of Interacting Sails through Viscous CFD”, *INNOVSail2008, Innovation in high performance sailing Yacht*, Lorient, France, May 2008.

23. Querard, A.B.G. and Wilson, P.A., “Aerodynamic of Modern Square Head Sails: A Comparative Study Between Wind-Tunnel Experiments and RANS Simulations”, *The Modern Yacht, 2007*, 107-114.

24. Spalart, P.R., Allmaras, S.R., “A one-equation turbulence model for aerodynamic flows”, AIAA paper 92-0439, 1992.

25. Gambit 2.3 & Fluent 6.2 users guide and tutorials, http://www.fluent.fr/

26. Wilkinson, S., “Partially Separated Flows around 2D Masts and Sails”, PhD Thesis, University of Southampton, UK, 1984.

27. Wilkinson, S., “Static Pressure Distributions over 2D mast/sail geometries”, Marine Technology 26, 4, 333-337, 1989.

28. Wilkinson, S., “Boundary Layer Explorations over a 2D mast/sail geometry”, Marine Technology 27, 4, 250-256, 1990.

29. Heppel P., “Accuracy in Sail Simulation: Wrinkling and Growing Fast Sails”, *Proceeding of the 2nd High Performance Yacht Design Conference*, Auckland, New-Zeeland, December 2002.

30. Barnes, M., “Form and stress engineering of tension structures”. Structural Engineering Review Vol 6 No 3-4 175-202, 1994.

31. Kamakoti, R. and Shyy, W., “Fluid-Structure Interaction for Aeroelastic Applications”, *Progress in Aerospace Sciences*, *40*, 535-558, 2004.

32. Desbrun, M., Meyer, M., Alliez, P., “Intrinsic Parameterizations of Surface Meshes”, Vol 21, N°2, Eurographics 2002.

33. Pulliam T.H., Nemec M., Holst T., Zingg D.W., “Comparison of Evolutionary (Genetic) Algorithm and Adjoint Methods for Multi-Objective Viscous Airfoil Optimizations, AIAA paper 2003-0298, Reno, USA,

34. Rechenberg, I., Evolutionstrategie – Optimierung technischer Systeme nach Prinzipien der Biologischen Evolution, PhD thesis, 1971, reprinted by Fromman-Holzboog in 1973.

35. Hansen, N. and A. Ostermeier (2001). Completely Derandomized Self-Adaptation in Evolution Strategies. *Evolutionary Computation*, 9(2), 2001.

36. Hansen, N. and S. Kern (2004). Evaluating the CMA Evolution Strategy on Multimodal Test Functions. In *Eighth International Conference on Parallel Problem Solving from Nature PPSN VIII, Proceedings*, pp. 282-291, Berlin: Springer, 2004.

37. Müller S.D., “Bio-Inspired Optimization Algorithms for Engineering Applications”, PhD thesis, Institute of Computational Science, ETH Zurich, 2002.

38. Jones P., & Korpus R., “International America’s Cup class yacht design using viscous flow CFD”, *SNAME 15th Chesapeake Sailing Yacht Symposium*, Annapolis, Maryland, USA, January 2001.

39. Bethwaite F., “High performance sailing”, Waterline Books, p209, 1996.

40. Rumsey, C.L. and Ying, S.X., “Prediction of high lift: review of the present CFD capability”, *Progress in Aerospace Sciences*, *38*, 145-180, 2002.

41. Marchaj C. A., *Sail Performance: Techniques to Maximize Sail Power*, McGraw Hill, Great Britain, 1996.

42. Deb, K., “An efficient constraint handling method for genetic algorithms”, *Computer Methods in Applied Mechanics and Engineering*, *186*, 311-338, 2000.

43. Chapin V.G., de Carlan N. & Heppel P., “A Multidisciplinary Computational Framework for Sailing Yacht Rig & Sails Design through Viscous FSI”, Chesapeake Sailing Yacht Symposium, Annapolis, 17-19 March 2011.

10. AUTHORS’ BIOGRAPHIES

Vincent G. Chapin, Associate Professor ISAE. Member of the “Advanced Aerodynamic & Control” team of the Aerodynamic Energetic and Propulsion Department of ISAE. His research is devoted to unsteady flows, flow control and innovating aerodynamic.

Nolwenn de Carlan, ENSICA engineer.

Peter Heppel, Engineer, specialist of non linear large displacement structures.